

7.0 CALIBRATION OF NOAA KLM INSTRUMENTS

The calibration of a satellite radiometer involves finding the transfer function between digital counts from the instrument and the scene input spectral radiance for all the instrument's spectral channels.

In the infrared region of the spectrum, calibration is accomplished by using accurate blackbodies in a thermal/vacuum (T/V) environment. A T/V chamber is used to avoid atmospheric effects and to better simulate the space environment in which the instrument must ultimately operate. The T/V chamber contains accurate extended area blackbody cavities which are used as infrared sources. Calibration traceability to the National Institute for Standards and Technology (NIST) is via the temperature of the blackbody.

In the visible region, calibration is performed on a test bench. No significant errors are introduced by performing the calibration in this manner. The laboratory source most used to calibrate visible channels is an integrating sphere. The integrating sphere is the device used to create a visible radiance which is traceable to the NIST. Calibration of the AVHRR and HIRS visible channels uses one 102 cm (40-in) sphere exclusively in order to aid inter-instrument calibration consistency.

In the ultraviolet region, calibration is performed using several calibrated standard lamps; a quartz-halogen lamp for use in the 250-400 nm range, an argon mini-arc for the 160-280 nm range and a deuterium (D₂) lamp covering the total spectral range. In the microwave region, calibration is performed in a T/V environment using calibrated blackbody radiometric sources.

Calibration updates to characterize the in-orbit performance of the visible and near-infrared channels of the AVHRR are introduced in the Level 1b data when necessary by NESDIS. The historical visible calibration notices are available under the NESDIS Special Bulletins section at <http://www.ssd.noaa.gov/PS/SATS/bulletins.html>.

The SEM-2 TED and MEPED responses are calibrated with particle (proton and electron) beams, with the results summarized in a Calibration Report for each instrument. The TED calibrated responses vary slightly from unit to unit, since the Continuous Dynode Electron Multiplier (CDEM) detectors have slightly varying detection efficiencies. The MEPED particle responses are essentially identical for all units. The TED and MEPED also have In-Flight Calibration cycles which verify the stability of the electronic gains, thresholds, channel logic, and detector noise.

7.1 AVHRR

The NOAA KLM Advanced Very High Resolution Radiometer, Version 3 (AVHRR/3), differs from AVHRR Versions 1 and 2 flown on the earlier POES satellites. . The AVHRR/3 is a six channel instrument, with three of the channels located in the visible and near-infrared regions of the spectrum, having effective wavelengths around 0.63 micrometers (channel 1), 0.86 micrometers (channel 2) and 1.6 micrometers (channel 3A), while the remaining three are located in the atmospheric window regions in the infrared with effective wavelengths centered around 3.7 micrometers (channel 3B), 10.8 micrometers (channel 4) and 11.5 micrometers (channel 5). Since quantitative radiometric applications of the AVHRR radiance measurements have become increasingly important both in research and operational environments, it has been

necessary to accurately calibrate the sensors in order that the AVHRR radiance measurements meet the stringent performance requirements necessitated by the accuracy requirements of the products derived from these radiances. For example, accuracies on the order of less than 2% are desired in the AVHRR radiances measured in channels 1, 2 and 3A. These radiances are used for improving the accuracy of atmospheric aerosol retrievals over the oceans in order that they may be used with confidence in atmospheric energy studies. Similarly, the well established need that sea surface temperatures determined using the brightness temperatures measured in channels 3B, 4 and 5 should be accurate to within a few tenths of a degree Kelvin for use in climate and global change studies. This need necessitated development of user friendly correction procedures for the non-linearities associated with the AVHRR thermal infrared channels and also imposes stringent requirements on the allowable noise-equivalent temperatures associated with the same.

Against this background, the procedures for the pre- and post-launch calibration of the different AVHRR channels are described. This description is based on the work performed at the NOAA/NESDIS Center for Satellite Applications and Research (STAR) and on the material furnished by ITT Aerospace/Communications Division, Fort Wayne, Indiana (the instrument manufacturer).

7.1.1 Visible and Near-Infrared Channels

7.1.1.1 Pre-launch Calibration

The visible and near-infrared channels of the AVHRR/3 were calibrated prior to launch at the facilities of ITT, following a protocol which has evolved over the past two decades. A 102 cm (40 in) diameter integrating sphere is used as the source of illumination. The integrating sphere is equipped with seventeen 45-W lamps and three 150-W lamps mounted in a ring pattern. The radiance emerging from the integrating sphere port which has a diameter of 35.6 cm (14 in), can be varied over three orders of magnitude by illuminating the sphere with a suitable combination of the various lamps. A separate 11.4 cm (4.5 in) diameter integrating sphere, equipped with a 45-W lamp and an aperture wheel, is used as the source when lower levels of illumination are desired. The level of illumination is varied in twenty-five steps for channel 1; sixteen steps for channel 2; and 11 steps for channel 3A. At each level of illumination of the integrating sphere, 3600 measurements of the signal issuing from the AVHRR when it views the sphere and the space clamp target are made, and the mean and standard deviation recorded, and converted to digital counts on a 10-bit scale. Generally, the AVHRR signals when it views the integrating sphere with all of the lamps turned off, and when it views the space clamp target (essentially a blackbody) are very close to each other.

The integrating sphere is periodically calibrated for its spectral output and linearity with an Optronic Laboratories Model OL750S Automated Spectroradiometer System and an Optronic Laboratories Model OL410 Integrating Sphere Standard; the Integrating Sphere Standard is traceable to radiance standards maintained at NIST. The uncertainty in the calibration of the 102 cm (40 in) integrating sphere source is estimated to be of the order of 5%.

It should be noted that the AVHRRs were calibrated at intervals not to exceed one year, until

they were launched. The last calibration was performed as close to the launch as practicable. Greater details of the pre-launch calibration of the AVHRR are found in Rao (1987).

It is the usual practice in NOAA to give the pre-launch calibration results in the form of a simple linear regression relationship between the measured AVHRR signal, C_{10} , expressed in ten-bit counts, and the albedo, A , of the integrating sphere source at different levels of illumination.

Thus,

$$A \equiv SC_{10} + I \quad (7.1.1.1-1)$$

Where S is the slope (percent albedo/count) and I is the intercept (percent albedo) listed in the Level 1b data under the heading “pre-launch”. **It should therefore be noted that the use of these slope and intercept values with the measured AVHRR will yield the albedo in percent under the assumption that the pre-launch calibration is valid in orbit.**

The albedo A (or the reflectance factored or scaled radiance) of the Earth scene is given by:

$$A(\text{percent}) = \frac{100\pi I}{F} \quad (7.1.1.1-2)$$

Where I and F are, respectively, the in-band radiance ($\text{W m}^{-2} \text{sr}^{-1}$) of the Earth scene and the extraterrestrial solar irradiance (W m^{-2}) at normal incidence at the top of the atmosphere at mean Earth-Sun distance, I and F are given by:

$$I = \int_{\lambda_1}^{\lambda_2} I_{\lambda} \tau_{\lambda} d\lambda \quad ((7.1.1.1-3)$$

And

$$F = \int_{\lambda_1}^{\lambda_2} F_{0\lambda} \tau_{\lambda} d\lambda \quad (7.1.1.1-4)$$

where τ_{λ} is the normalized response of the instrument at the wavelength λ , I_{λ} is the radiance ($\text{W m}^{-2} \text{sr}^{-1} \text{:m}^{-1}$) and $F_{0\lambda}$ is the extraterrestrial solar irradiance ($\text{W m}^{-2} \text{:m}^{-1}$) at the wavelength λ ; where λ_1 and λ_2 are the lower and upper cut-off wavelengths of the channel. Other quantities are the equivalent width ω (:m) and the effective wavelength λ_e given by:

$$\omega = \int_{\lambda_1}^{\lambda_2} \tau_{\lambda} d\lambda \quad (7.1.1.1-5)$$

And

$$\lambda_e = \frac{\int_{\lambda_1}^{\lambda_2} \lambda F_{0\lambda} \tau_{\lambda} d\lambda}{F} \quad (7.1.1.1-6)$$

It should be noted that the albedo calculated using Equation 7.1.1.1-2 shows a small but finite

variation with the extraterrestrial solar irradiance spectra used in the calculation of F. It is thus preferable to work with the in-band radiance I or the radiance I_8 ; however, these quantities are not included in the Level 1b data stream.

A salient feature of the AVHRR/3 is the use of dual gain detection circuitry in the visible and near-infrared channels to enhanced radiometric resolution at the lower end of the dynamic range of the albedo; this results in minor losses in resolution at the higher values of albedo. The dual gain settings for channels 1, 2 and 3A are given in Table 7.1.1.1-1 below.

Channel	Albedo range (percent)	Counts
1 and 2	1-25	0-500
	26-100	501-1000
3A	1-12.5	0-500
	12.6-100	501-1000

The dual gain feature necessitates the use of two sets of slope and intercept values for channels 1, 2 and 3A to accommodate the two gain ranges. Thus, the Level1b data has, in addition to the prelaunch calibration coefficients, two sets of slope and intercept values for each of the three channels based on post-launch calibration (see next section). These are listed under the heading “operational” in the Level 1b data stream.. As mentioned earlier, since these slope and intercept values are in the albedo (or reflectance factor or scaled radiance) representation, use of the same with the AVHRR Earth scene signal will yield the albedo (in percent). The dual gain cross-over point is defined as the count value at which both the high and low range regression equations for the albedo A will yield the same value of the albedo. The cross-over point was determined using the pre-launch integrating sphere and the electronic calibration ramp. The user can find the slope and intercept values, and the values of F, o, and δ_e in Appendix D.

7.1.1.2 Post Launch Calibration

The visible and near-infrared channels of the TIROS-N series of AVHRRs were known to degrade in orbit and similar degradations were observed in Channels 1, 23a of the NOAA KLM AVHRR/3.

The absence of on board calibration devices for these channels necessitated the development of vicarious techniques for post-launch calibration. Accordingly, vicarious calibration techniques that have been developed (e.g. Rao and Chen 1995) to characterize the post-launch performance of Channels 1 and 2 of the TIROS-N AVHRRs, were adapted to the AVHRR/3. These techniques use radiometrically stable terrestrial calibration target sites and congruent path aircraft/satellite measurements to monitor the calibration of the instrument as a function of time. These techniques have been modified to account for the split-gain feature of the instrument.

7.1.2 Thermal Infrared Channels (channels 3B, 4 and 5)

7.1.2.1 Pre-launch Calibration

Pre-launch calibration of the infrared channels was carried out in a thermal vacuum chamber to simulate conditions in space. The radiometer sequentially views three blackbody targets, a cold target ($\approx 95K$) representing cold space, an external laboratory blackbody representing “Earth”, and its own warm blackbody, the internal calibration target (ICT). The sequence is the same as show in Figure 7.1.2.2-1. All blackbody sources have calibrations traceable to NIST. The internal and external blackbody temperatures are measured by Platinum Resistance Thermometers (PRTs). From these temperatures, AVHRR radiances for each thermal channel are computed. The AVHRR outputs 10-bit count values, integers in the 0-1023 range. The detection circuits for these channels are such that count output increases when incoming radiance decreases.

The entire pre-launch calibration test cycle was repeated on three, four or five separate days. Each day, the instrument operating temperature (measured by the PRTs) was fixed at a different value in the 10, 15, 20, 25 and 30C range for the entire cycle. This range brackets the range of operating temperatures encountered in orbit. For each calibration run, temperature (radiance) and count data were collected as the laboratory blackbody cycled through 15-17 temperature plateaus between 180 K and 335 K, which spans the entire range of Earth target temperatures.

7.1.2.2 In-orbit Calibration Overview

During each in-orbit scan line, the AVHRR views three different types of targets, as shown in Figure 7.1.2.2-1. It first outputs 10 counts when it views cold space, then a single count for each of the 2,048 Earth targets (pixels), and finally 10 counts when it views the internal blackbody target. (Only the AVHRR scan mirror actually rotates). The cold space and internal blackbody target views are used to calibrate the AVHRR, because a radiance value can be independently assigned to each target.

Figure 7.1.2.2-1. AVHRR Thermal Channel Calibration Sequence.

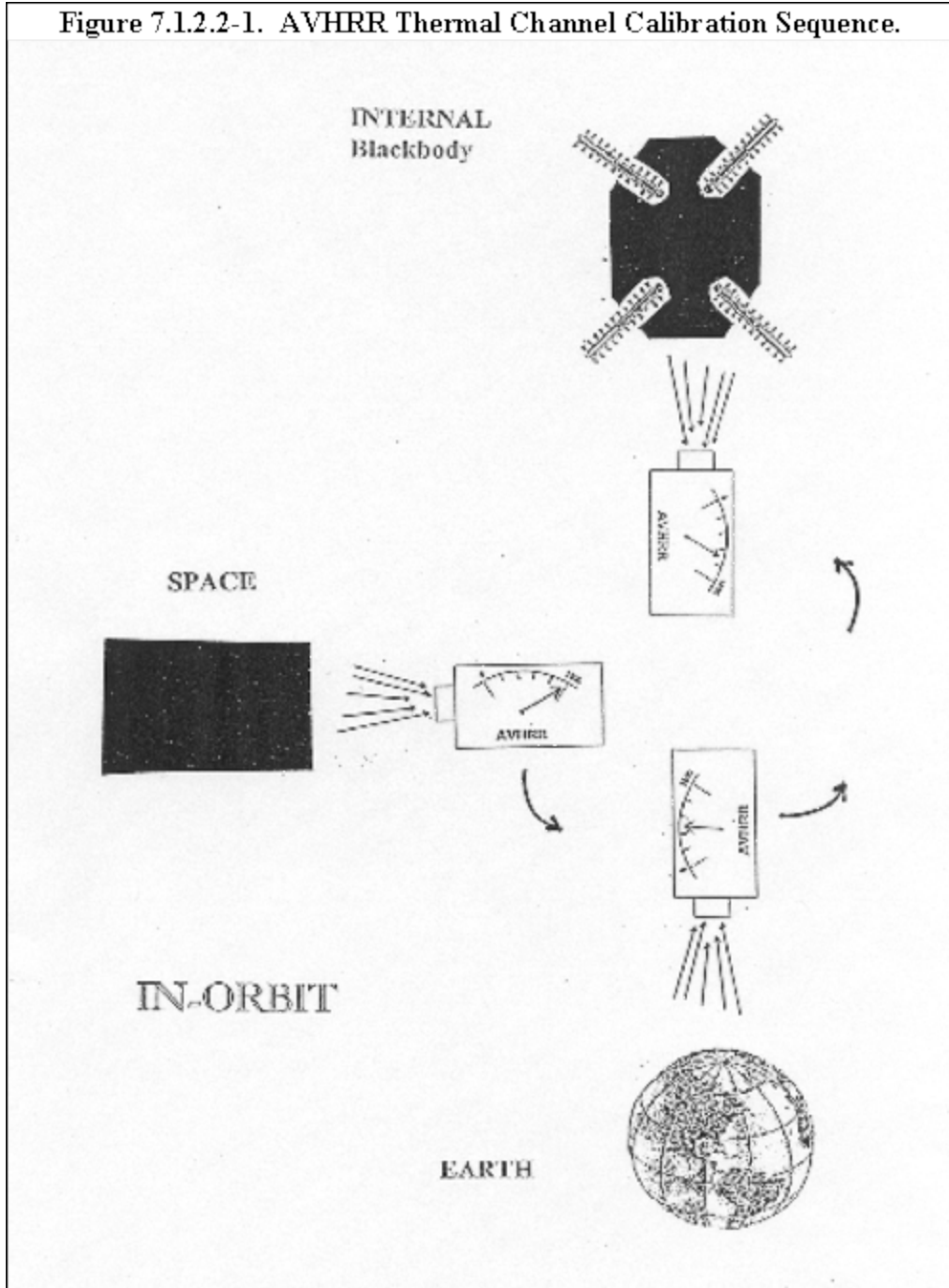


Figure 7.1.2.2-1. AVHRR Thermal Channel Calibration Sequence

The internal blackbody temperature T_{BB} is measured by four Platinum Resistance Thermometers (PRTs) embedded in the AVHRR instrument. The radiance N_{BB} received by the AVHRR from the internal blackbody in each thermal channel is computed from T_{BB} the spectral response (filter) function of each channel. The radiance of space value N_S , designed to accurately account for pre-launch information, and is computed from pre-launch data. These radiances, together with the average space count C_S and average blackbody count C_{BB} provide two points (C_{BB} , N_S) on the radiance versus count graph. A straight line drawn between the two points generates the

linear radiance versus count estimate. The AVHRR count output C_E from viewing an Earth target is substituted into the linear equation and produces linear radiance N_{LIN} . Pre-launch measurements indicate that the actual radiance versus count graph is quadratic so N_{LIN} is input into a quadratic equation, defined by pre-launch measurements, to give the nonlinear radiance correction N_{COR} . The incoming radiance N_E from the Earth target that causes AVHRR output count value C_E is found by adding N_{COR} to N_{LIN} . An equivalent blackbody temperature T_E can be computed from Earth radiance value N_E .

7.1.2.3 Steps to Calibrate the AVHRR Thermal Channels (Level 1b Data Users)

Starting with the NOAA-15 (NOAA-K) satellite, NESDIS incorporated the nonlinear radiance corrections for AVHRR thermal channels 4 and 5 into the Level 1b data stream. The corrections are in the GAC and LAC datasets, and also in the HRPT datasets produced operationally by NESDIS. Users compute the scene radiance, N_E in units of $mW/(m^2-sr-cm^{-1})$ from the 10-bit earth-scene count, C_E , by the formula:

$$N_E = a_0 + a_1 C_E + a_2 C_E^2 \quad (7.1.2.3-1)$$

There is one set of coefficients for each thermal channel 3B, 4 and 5 in the NOAA KLM Level 1b dataset. The channel 3B detector responds linearly to incoming radiance so for channel 3B the coefficient a_2 will always be 0. Section 8 contains format information about how the Level 1b data are stored. The coefficient a_0 for AVHRR channel 4 is specified as "IR Operational Cal Ch4 Coefficient 1"; etc

As a numerical example, suppose $C_E = 410$ for Channel 4, and $a_0 = 155.58$, $a_1 = -0.1668$ and $a_2 = 0.000010$, then,

$$N_E = 155.58 - 0.1668 \times 410 + 0.000010 \times (410)^2 = 88.9 \text{ mW}/(m^2-sr-cm^{-1})$$

To convert the computed Earth scene radiance value N_E into an equivalent black body temperature value T_E , use the two-step process defined by Equations 7.1.2.4-8 and 7.1.2.4-9 in section 7.1.2.4.

The constants for converting radiance to black body temperature are also found in the Level 1b LAC and GAC Header Records, but in a slightly different form. In Tables 8.3.1.3.2-1 and 8.3.1.4.2-1 (for LAC and GAC data, respectively), under the heading radiance conversion (octets 281-328), channels 3B, 4 and 5 each have three sets of constants; these constants are called central wavenumber, constant1 and constant2. The central wavenumber value Λ_c is used in Equation 7.1.2.4-8 to calculate T_E^* , and the blackbody temperature T_E is computed by the formula:

$$T_E = \text{constant1} + (\text{constant2}) T_E^*$$

7.1.2.4 Steps to Calibrate the AVHRR Thermal Channels (HRPT Receiving Station Data Users)

Step 1. The temperature of the internal blackbody target is measured by for PRTs. In each scanline, data words 18, 19 and 20 in the HRPT minor frame format contain three readings from one of the four PRTs. (See Section 4.1.3) A different PRT is sampled each scanline; every fifth scanline all three PRT values are set equal to 0 to indicate that a set of four PRTs has just been sampled. The count value C_{PRT} of each PRT is converted to temperature T_{PRT} by the formula

$$T_{PRT} = d_0 + d_1 C_{PRT} + d_2 C_{PRT}^2 + d_3 C_{PRT}^3 + d_4 C_{PRT}^4 \quad (7.1.2.4-1)$$

The coefficients d_0 , d_1 , d_2 , d_3 and d_4 vary slightly for each PRT. Values for the coefficients are found in Appendix D, in Table D.1-8 for NOAA-15 (coefficients d_3 and d_4 are 0 for NOAA-15), Table D.2-9 for NOAA-16, Table D.3-3 for NOAA-17 and Table D.4-3 for NOAA-18. To calculate the internal blackbody temperature T_{BB} , NESDIS uses the simple average

$$T_{BB} = \frac{(T_{PRT1} + T_{PRT2} + T_{PRT3} + T_{PRT4})}{4} \quad (7.1.2.4-2)$$

Step 2. The radiance N_{BB} sensed in each thermal AVHRR channel from the internal blackbody at temperature T_{BB} is the weighted mean of the Planck function over the spectral response of the channel. The spectral response function for each channel is measured in approximately 200 wavelength intervals and provided to NESDIS by the instrument manufacturer. In practice, a look-up table relating radiance to temperature is generated for each channel. Each table specifies the radiance for every tenth of a degree (K) between 180 and 340K. The tables are referred to as “Energy Tables”. It has been found that the following two-step equation accurately reproduces Energy Table equivalent blackbody temperatures to within $\forall 0.01K$ in the 180 to 340K range. Each thermal channel has one equation, which uses a centroid wavenumber Λ_c and an “effective” blackbody temperature T_{BB}^* . The two steps are:

$$T_{BB}^* = A + BT_{BB} \quad (7.1.2.4-3)$$

$$N_{BB} = \frac{c_1 \nu_e^3}{\frac{c_2 \nu_c}{e^{T_{BB}^*}} - 1} \quad (7.1.2.4-4)$$

Where the first and second radiation constants are:

$$c_1 = 1.1910427 \times 10^{-5} \text{ mW}/(\text{m}^2\text{-sr-cm}^{-4})$$

$$c_2 = 1.4387752 \text{ cm-K.}$$

The values for Λ_c and the coefficients A and B for channels 3B, 4 and 5 are unique for each spacecraft and are found in Appendix D; Table D.1-11 for NOAA-15, Table D.2-12 for NOAA-16, Table D.3-7 for NOAA-17 and Table D.4-7 for NOAA-18. The single centroid wavenumber for each channel replaces the method for previous AVHRRs, which used a different central wavenumber in each of four temperature ranges. In the previous version of this documentation,

the A coefficients in Tables D.1-11 and D.2-12 were minus numbers and the B coefficients were slightly greater than one. They were used to convert radiance into equivalent blackbody temperature, and converted “effective” temperature T_{BB}^* into T_{BB} , instead of the reverse way as shown in Equation 7.1.2.4-3.

Step 3. Output from the two in-orbit calibration targets is used to compute a linear estimate of the Earth scene radiance N_E . Each scanline, the AVHRR views the internal blackbody target and outputs 10 count values for each of the three thermal channel detectors; these are found in words 23 to 52 in the HRPT data stream. When the AVHRR views cold space, 10 counts from each of the five channel sensors are output and placed into words 52 to 102. (Table 4.1.3-1 describes how these data are multiplexed.) Count values for each channel are averaged together to smooth our random noise; often counts from five consecutive scanlines are averaged because it takes five lines to obtain a set of all four PRT measurements. The average blackbody count C_{BB} and the average space count C_S , together with blackbody radiance N_{BB} and space radiance N_S , explained in the next paragraph, are used to compute the linear radiance estimate N_{LIN} ,

$$N_{LIN} = N_S + (N_{BB} - N_S) \frac{(C_S - C_E)}{(C_S - C_{BB})} \quad (7.1.2.4-5)$$

where C_E is the AVHRR count output when it views one of the 2,048 Earth targets.

The detector in thermal channel 3B has a linear response to incoming radiance so the linear radiance computed from Equation 7.1.2.4-5 is the correct value for channel 3B. For this channel, the radiance of space value N_S is actually = 0; no nonlinear corrections need to be made.

The Mercury-Cadmium-Telluride detectors used for channels 4 and 5 have a nonlinear response to incoming radiance. Pre-launch laboratory measurements show that:

- a. scene radiance is a slightly nonlinear (quadratic) function of AVHRR output count,
- b. the nonlinearity depends on the AVHRR operating temperature.

It is assumed that the nonlinear response will persist in orbit. For the NOAA KLM series of satellites, NESDIS uses a radiance-based nonlinear correction method. IN this method, the linear radiance estimate is first computed using a non-zero radiance of space, the N_S term in Equation 7.1.2.4-5. Then, the linear radiance value is input into a quadratic equation to generate the nonlinear radiance correction N_{COR} :

$$N_{COR} = b_0 + b_1 N_{LIN} + b_2 N_{LIN}^2 \quad (7.1.2.4-6)$$

Finally, the Earth scene radiance is obtained by adding N_{COR} to N_{LIN} ,

$$N_E = N_{LIN} + N_{COR}$$

Introducing the non-zero radiance of space value is a mathematical device which has two primary advantages. First, only one quadratic correction equation per channel is necessary; the

quadratic coefficients are independent of AVHRR operating temperature. Second, the method reproduces pre-launch measurements very well; RMS differences between the fitted data and the measured data are approximately 0.1K for both channels 4 and 5. Values for N_S and the quadratic coefficients b_0 , b_1 and b_2 are found in Appendix D, Table D.1-14 for NOAA-15, and Table D.2-15 for NOAA-16, Table D.3-2 for NOAA-17 and Table D.4-2 for NOAA-18.

Step 4. Data users often convert the computed Earth scene radiance value N_E into an equivalent blackbody temperature T_E . This temperature is defined by simple inverting the steps used to calculate the radiance N_E sensed by an AVHRR channel from an emitting blackbody at a temperature T_E . The two-step process is:

$$T_E^* = \frac{c_2 \nu_c}{\ln \left[1 + \left(\frac{c_1 \nu_c^3}{N_E} \right) \right]} \quad (7.1.2.4-8)$$

$$T_E = \frac{T_E^* - A}{B} \quad (7.1.2.4-9)$$

The values for Λ_c and the coefficients A and B are again found in appendix D; Table D.1-11 for NOAA-15, Table D.2-12 for NOAA-16, Table D.3-7 for NOAA-17 and Table D.4-7 for NOAA-18.

7.1.2.5 Summary of Calibration Equations for HRPT Users

Compute the blackbody temperature:

$$\begin{aligned} T_{PRT1} &= d_0 + d_1 C_{PRT1} + d_2 C_{PRT1}^2 + d_3 C_{PRT1}^3 + d_4 C_{PRT1}^4 \\ T_{PRT2} &= d_0 + d_1 C_{PRT2} + d_2 C_{PRT2}^2 + d_3 C_{PRT2}^3 + d_4 C_{PRT2}^4 \\ T_{PRT3} &= d_0 + d_1 C_{PRT3} + d_2 C_{PRT3}^2 + d_3 C_{PRT3}^3 + d_4 C_{PRT3}^4 \\ T_{PRT4} &= d_0 + d_1 C_{PRT4} + d_2 C_{PRT4}^2 + d_3 C_{PRT4}^3 + d_4 C_{PRT4}^4 \end{aligned}$$

$$T_{BB} = \frac{(T_{PRT1} + T_{PRT2} + T_{PRT3} + T_{PRT4})}{4}$$

Compute the blackbody radiance:

$$T_{BB}^* = A + BT_{BB}$$

$$N_{BB} = \frac{c_1 \nu_e^3}{\frac{c_2 \nu_e}{e^{T_{BB}^*}} - 1}$$

Compute the Earth view radiance using the nonlinearity correction:

$$N_{LIN} = N_S + (N_{BB} - N_S) \frac{(C_S - C_E)}{(C_S - C_{BB})}$$

$$N_{COR} = b_0 + b_1 N_{LIN} + b_2 N_{LIN}^2$$

$$\begin{aligned} N_E \\ = N_{LIN} + N_{COR} \end{aligned}$$

Convert Earth view radiance to equivalent blackbody temperature:

$$T_E^* = \frac{c_2 \nu_e}{\ln \left[1 + \left(\frac{c_1 \nu_e^3}{N_E} \right) \right]}$$

$$T_E = \frac{T_E^* - A}{B}$$

7.2 HIRS/3

For each internal target PRT, the averaged counts are transformed to temperatures by a quadratic relation. The four temperatures, or those that are deemed to be operating properly, are averaged.

For each thermal channel (1-19, or all telemetry channels except number 12) the blackbody radiance can be computed from the Planck relation,

$$r = \frac{c_1 \nu^3}{\left[\exp \left(\frac{c_2 \nu}{T^*} \right) - 1 \right]}$$

using central wavenumbers, Λ , computed prior to the launch of the satellite, and an "apparent" temperature defined by

$$T^* = b + c T$$

where b and c are channel dependent coefficients (the so-called band-correction coefficients) computed before the launch of the satellite, and T is the averaged temperature of the internal target. The two constant terms in the Planck relation is $c_1 = 1.1910659 \times 10^{-5} \text{ mW}/(\text{m}^2\text{-sr-cm}^{-4})$ and $c_2 = 1.438833 \text{ cm-K}$.

During the calibration cycle, the counts for the space and internal target views are each averaged, using a 3σ throw out criterion, over the range of the 56 measurements deemed to be free from scan mirror movement and other unsatisfactory conditions. If any positions are systematically deleted from one, they will also be deleted from the other.

Assuming that radiance can be related to counts through the quadratic:

$$r = a_0 + a_1 C_\Lambda + a_2 C_\Lambda^2$$

where r is radiance, C_v is the output in counts from the view, and a_0 , a_1 and a_2 are constants. Before launch, a_2 is computed and the assumption is made that this is an unchanging characteristic of the channel.

Now the coefficients a_0 and a_1 can be determined. Equation 7.2-3 is applied to the views of space and the internal target, yielding:

$$0 = a_0 + a_1 C_\Lambda + a_2 C_\Lambda^2 \quad (7.2-3)$$

and

$$r_b = a_0 + a_1 C_b + a_2 C_b^2, \quad (7.2-5)$$

where C_s and C_b are the mean counts from the views of space and the internal target, respectively, and r_b is the radiance of the internal target. Or, since a_2 is known,

$$-a_2 C_s^2 = a_0 + a_1 C_s \quad (7.2-6)$$

$$r_b - a_2 C_b^2 = a_0 + a_1 C_b \quad (7.2-7)$$

Then the slope and intercept become:

$$a_1 = \frac{[r_b - a_2(C_b^2 - C_s^2)]}{(C_b - C_s)} \quad (7.2-8)$$

$$a_0 = -a_2 C_s^2 - a_1 C_s \quad (7.2-9)$$

Nominally, the slope and the intercept can be determined from simultaneous views of space and the internal blackbody source. As discussed below, only the intercept varies appreciably

throughout an orbit, the linear and quadratic terms being essentially constant.

The HIRS/3 instrument measures all radiation falling on the detector. That is, it is a total radiometer. To minimize false fluctuations in the signals, the instrument temperature is carefully controlled, so that most optical components experience temperature changes very slowly with respect to the times between calibration cycles (256 seconds). However, the baffle (identified as the secondary mirror) is a blackened light material which is subject to short-term temperature changes from emission or blackbody radiation and absorption of incident radiation from the internal blackbody source (about 280 K), space (2.73 K), and the variable earth views (about 200-275 K plus reflected sunlight). The result is that the contribution by the baffle affects all measurements on a time scale of seconds and this must be accounted for.

At every line, the secondary mirror temperature is linearly interpolated to the midpoint of the radiometric data (beam position 28.5) according to:

$$T_{snn}' = T_{snn-01} + 0.4609(T_{snn} - T_{snn-01}) \quad (7.2-10)$$

where nn is the line number in the superswath (00 to 39), nn-01 is the previous line, and T_s is the measurement of the secondary mirror temperature. In the first line of an orbit the value

$$T_{snn}' = T_{snn} - 0.5391(T_{snn+1} - T_{snn})$$

is used. The interpolated values are preserved during the processing of a superswath (40 values plus the value from the last line of the previous superswath).

It is assumed that the slopes do not change appreciably over a 24-hour period, varying only about one part in 8000 throughout an orbit. During each 24 hours, the slopes are saved (about 19 times 350 values) and are averaged,

$$\overline{a_{100}}'' = \frac{1}{N} \sum_{i=1}^{i=N} a_{li} \quad (7.2-12)$$

where N is the number of slopes, i is an index, and a_1 is a slope defined in Eq. 7.2-8. A 3σ throw-out criterion is used. After the average is computed, the accumulated slopes are purged. The averaged values are used during the next 24 hours, during which a new group of slopes is accumulated (a rotating file is undesirable).

To account for variations in the temperature of the telescope baffle, the intercepts at the time of the calibration are related to the baffle temperature through the relation:

$$a_{000} = b_0 + b_1 T_{s00}' \quad (7.2-13)$$

where T_{s00}' is the interpolated secondary mirror (baffle) temperature in line 00 (space view). The constants b_0 and b_1 are evaluated when this equation is solved by least squares from intercepts and interpolated secondary mirror temperature accumulated during 24 hours (about 350 values of each), using a 3σ throw-out criterion. Only the term b_1 is used hereafter. It is applied during the following 24 hours.

At each calibration cycle, intercepts are recomputed from the mean space counts and the averaged slopes,

$$a_{000}'' = -\overline{a_{100}''} C_{s00} - a_2 C_{s00}^2 \quad (7.2-14)$$

where the value a_{000}'' is used at the time of the space view, $\overline{a_{100}''}$ is the mean slope, and C_{s00} is the mean of the space counts in line 00.

Only the averaged slopes are applied to the earth-viewing data. The intercepts must be interpolated between calibration cycles by using the secondary mirror temperature:

$$a_{0nn}'' = a_{000}'' + nn \frac{(a_{040}'' - a_{000}'')}{40} + b_1 \left[(T_{snn}' - T_{s00}') - \frac{nn (T_{s40}' - T_{s00}')}{40} \right] \quad (7.2-15)$$

where nn is a scan line number in a superswath numbered 00-39; $nn = 40$ refers to $nn = 00$ of the next superswath.

For partial superswaths at the start and end of an orbit the intercepts are computed according to

$$a_{0nn}'' = a_{0xx}'' + b_1 (T_{snn}' - T_{sxx}') \quad (7.2-16)$$

where the subscript xx refers to the nearest calibration cycle ($xx = 40$ or 00 , respectively).

The initial values of b_1 immediately after launch will be derived from current data from another satellite or will be zeroes (optional). The initial values of the mean slopes immediately after launch will be from another satellite or from data for a single orbit (optional). Data in the Level 1b files derived from use of these initial data will be excluded from the archive; that is, they will be excluded for at least 24 hours after processing begins.

The HgCdTe detector used in the HIRS/3 instrument operates in the photoconductive mode and is slightly nonlinear in its response to radiative flux. Adjustments for nonlinear response are made in Eqs. 7.2-8, 7.2-9, and 7.2-14. The coefficients a_2 are computed from test data taken by the fabricator of the instrument, and will not change throughout the lifetime of the instrument. The combined coefficients will be saved in the Level 1b data and will be applied to earth

measurements.

In summary, for the thermal channels:

a. During an orbit, accumulate

(1) The Channel 1-19 radiances for the blackbody temperatures at the time of the internal target views,

(2) The means and standard deviations of the space counts and the blackbody counts (in scan lines 00 and 01) for each channel, and

(3) The interpolated secondary mirror temperatures (Eqs. 7.2-10 and 7.2-11).

b. Compute the slopes and intercepts from the radiances and counts in according to Eqs. 7.2-8 and 7.2-9. Save both coefficients in temporary 24-hour files, along with the interpolated secondary mirror temperatures.

c. Once per day, compute the relation between intercepts and secondary mirror temperatures from a least-squares solution to Eq. 7.2-13, using a 3σ throw-out criterion.

d. Once per day, compute the average slopes over the previous 24-hour period, using a 3σ throw-out criterion. These are the slopes to be used during the subsequent 24 hours. After steps c. and d., the accumulated slopes will be purged.

e. Recompute the intercepts according to Eq. 7.2-14 at the time of the space views, $n = 00$.

f. Return to the start of the orbit or superswath and interpolate (which requires the recomputed intercept at the next space view) or extrapolate the intercepts for the times of the earth views (lines 02-39) according to Eqs. 7.2-15 or 7.2-16. Note that the starting point for all coefficients is line 00. For an incomplete superswath at the start of an orbit, the reference is line 40 (line 00 of the second superswath).

g. Compute earth-viewed radiances according to Eq. 7.2-3.

The calibration coefficients for Channel 20 (telemetry Channel 12) will be furnished by the fabricator of the instrument and will not change during the lifetime of the satellite.

The mean slopes, the interpolated intercepts, and the quadratic term will be the calibration coefficients appended to scan lines 02-39 of the Level 1b data; the 00 line will have zeroes; and line 01 will have the slope and intercept computed at the time of the calibration, a_{000} " (Eq. 7.2-14). Data encompassing a flagged calibration cycle (the preceding and current superswaths) are considered to be unusable, the calibration coefficients in lines 02-39 will be set to zero, and the Level 1b data will be properly flagged as unusable.

Logical records of Level 1b data will contain an even number of 8-bit bytes, and all logical records in the archive, regardless of purpose, will be the same length.

7.3 AMSU-A and AMSU-B

The Advanced Microwave Sounding Unit-A (AMSU-A) is a fifteen-channel total power microwave radiometer in two separate units: A1 and A2. The AMSU-A2, which has its own antenna system, contains Channels 1 and 2 at 23.8 and 31.4 GHz, respectively. The AMSU-A1, which consists of the two antenna systems A1-1 and A1-2, contains Channels 3-14 in the range of 50.3 - 57.29 GHz and Channel 15 at 89.0 GHz. Between the two antenna systems, A1-2 provides Channels 3, 4, 5, and 8 whereas A1-1 furnishes Channels 6, 7, and 9-15. Each of the AMSU-A antenna systems is required to have a nominal field-of-view (FOV) of 3.3 degrees $\pm 10\%$ at the half-power points and covers a crosstrack scan of ± 48 degrees 20 minutes (to beam centers) from the nadir direction with 30 Earth FOVs per scan line. The data received from the spacecraft will contain separate telemetry for each antenna system. Once every 8 seconds, the AMSU-A measures 30 Earth views, the space view twice and the internal blackbody target twice. Combination of Gunn diode cavity-stabilized and phase-locked loop oscillators (PLLO) are used to provide channel frequency stability. Channels 9-14 have both primary and secondary phase-locked loop oscillators (called PLLO#1 and PLLO#2, respectively) built-in. The PLLO#2 will be used for backup if the PLLO#1 fails. Gunn diode oscillators are used in other channels without backups. The output signals of these radiometric samples are digitized by 15-bit analog-to-digital converters.

The AMSU-B is a five-channel total power microwave radiometer with two channels centered nominally at 89 GHz and 150 GHz, and the other three centered around the 183.31 GHz water vapor line with double-sideband centers located at 183.31 ± 1 , ± 3 , and ± 7 GHz, respectively. AMSU-B has a FOV of 1.1 degrees $\pm 10\%$, and once every 8/3 seconds it measures 90 Earth views, four space views and four internal blackbody target views.

The calibration procedures for the AMSU-A and AMSU-B are the same, except a few minor differences to allow for the separate antenna systems. Table 7.3-1 lists the main differences between the AMSU-A and AMSU-B procedures. Radiances for both AMSU-A and -B Earth views are derived from the measured counts and the calibration coefficients inferred from the internal blackbody and space view data. Both AMSU-A and AMSU-B were tested and calibrated in T/V chambers before launch and the scanings of both instruments are synchronized to an 8-second pulse. Each instrument has four options for the viewing direction of the space view which can be selected by ground command, and one will be chosen immediately after launch. Note: The Calibration Parameters Input Data Sets (CPIDS) are included in the Header Records of Level 1b data according to the Header Record Format.

Table 7.3-1. Differences between the AMSU-A and AMSU-B procedures			
Items	AMSU-A	AMSU-B	Remarks

	A1-1	A1-2	A2		
Number of PRTs in each warm target	5	5	7	7	Internal black body targets
Number of Earth views per scan line	30	30	30	90	In-orbit
Blackbody and space samples	2	2	2	4	Per scan line
Definition of instrument temperature	RF Shelf A1-1	RF Shelf A1-2	RF Shelf A2	Mixer temp. of Ch. 18-20	Available in housekeeping
Backup of instrument temperature	RF Mux A1-1	RF Mux A1-2	RF Mux A2	Mixer temp of Ch. 16	See Note 1.
Secondary PLLO	Ch. 9-14	NO	NO	NO	Backup PLLO

Note 1: These temperatures (available in the housekeeping data) will be used as backups if the primary ones fail.

7.3.1 BLACKBODY TEMPERATURE

The physical temperatures of the internal blackbody targets are measured by Platinum Resistance Thermometers (PRTs). The number of PRTs used to measure the physical temperatures of the internal blackbody targets in each antenna system is given in Table 7.3-1. These PRTs, which were calibrated by individual manufacturers against ‘standard’ ones traceable to NIST, measure temperatures of the internal blackbody targets with an accuracy of $\pm 0.1\text{K}$. The outputs to the telemetry are PRT counts, which must be converted to PRT temperatures. The normal approach for deriving the PRT temperatures from counts is a two-step process, in which the resistance of each PRT (in ohms) is computed by a count-to-resistance look-up table provided by its manufacturer. Then, the individual PRT temperature (in degrees) is obtained from an analytic PRT equation. However, this can be compressed to a single step with negligible errors.

This single step process, which will be used with the NOAA KLM satellites, computes the PRT temperatures directly from the PRT counts, using a polynomial of the form

$$T_k = \sum_{j=0}^3 f_{kj} C_k^j \quad (7.3.1-1)$$

where T_k and C_k represent the temperature and count of the PRT. The coefficients, f_{kj} , will be provided for each PRT. Equation 7.3.1-1 is also used for other housekeeping temperature sensors, such as the mixers, the IF amplifiers and the local oscillators.

The mean blackbody temperature, T_w is a weighted average of all PRT temperatures:

$$T_w = \frac{\sum_{k=1}^m w_k T_k}{\sum_{k=1}^m w_k} + \Delta T_w \quad (7.3.1-2)$$

where m represents the number of PRTs for each antenna system as listed in Table 7.3-1. The w_k is the weight assigned to each PRT and ΔT_w is the warm load correction factor for each channel derived from the T/V test data for three instrument temperatures (low, nominal, and high). Values for ΔT_w will be provided for each instrument. For AMSU-A1-1, ΔT_w values for both PLLO#1 and PLLO#2 will be provided. The w_k value, which equals 1 (0) if the PRT is determined good (bad) before launch, will be provided for each flight model. If any of the PRT temperatures, T_k , differs by more than 0.2K from its value in the previous scan line, then the T_k should be omitted from the average in Equation 7.3.1-2.

Similarly, a cold space temperature correction, ΔT_c , is also provided for processing the in-orbit data. This is due to the fact that the space view is contaminated by radiation which originates from the spacecraft platform and the Earth's limb. Thus, the effective cold space temperature is given by,

$$T_c = 2.73 + \Delta T_c \quad (7.3.1-3)$$

where 2.73K is the cosmic background brightness temperature. The ΔT_c , which represents the contribution from the antenna side lobe interference with the Earth limb and spacecraft, is estimated initially for individual channels, but its optimal value will be determined from post-launch data analysis.

7.3.2 CALIBRATION COUNTS

For each scan, the blackbody counts C_w are the averages of two (four) samples of the internal black body in AMSU-A (AMSU-B). If any two samples differ by more than a preset limit of blackbody count variation ΔC_w (the initial limit is set to 3σ , where the standard deviation, σ , is calculated from the pre-launch calibration data C_w for each channel), the data in the scan should not be used.

Similarly, the space counts C_c are the average of two (four) samples of the space view for AMSU-A (AMSU-B). If any two space view samples differ by more than the preset limit, the data in the scan should be excluded.

To reduce noise in the calibrations, the C_x (where $x = w$ or c) for each scan line will be convoluted over several neighboring scan lines according to a weighting function:

$$\overline{C}_x = \frac{1}{n+1} \left[\sum_{i=-n}^n \left(1 - \frac{|i|}{n+1} \right) C_x(t_i) \right], \text{ counts} \quad (7.3.2-1)$$

the time of the current scan line, one can write $t_i = t_0 + i\Delta t$, where $\Delta t = 8$ seconds for AMSU-A and $8/3$ seconds for AMSU-B. The $2n+1$ values are equally distributed about the scan line to be where t_i (when $i \neq 0$) is the time of the scan line just before or after the current scan line. If t_0 is calibrated. For both AMSU-A and AMSU-B, the value of $n=3$ is recommended.

For the first and the last three scan lines in a file, the convolution of C_x should be omitted and the counts C_x from the individual scan line will replace \overline{C}_x . In the case of missing scan lines in the $2n+1$ interval, any one of the remaining scan lines can be selected to replace the missing one(s) in the convolution of C_x . If the gap of missing scans is larger than $2n+1$ (i.e., 7), the convolution process must be terminated at the beginning of the gap and starts anew at the end of the gap.

7.3.3 EARTH VIEW RADIANCES

The following calibration algorithm, which takes into account any nonlinear contribution due to an imperfect square law detector, is employed to convert observed Earth-viewing counts to radiances:

$$R_s = R_w + \frac{C_s - \overline{C}_w}{G} + Q, \frac{mW}{m^2 - sr - cm^{-1}} \quad (7.3.3-1)$$

where R_s is the scene radiance and R_w and R_c are the Planck radiances corresponding to the blackbody temperature T_w and the effective cold space temperature T_c defined in Equations 7.3.1-2 and 7.3.1-3, respectively. The C_s is the radiometric count from the scene (Earth) target. The averaged blackbody and space counts, \overline{C}_w and \overline{C}_c , are defined by Equation 7.3.2-1. The channel gain G and the quantity Q , which contains the quadratic contributions, are given by:

$$G = \frac{\overline{C}_w - \overline{C}_c}{R_w - R_c}, \frac{\text{counts}}{mW / (m^2 - sr - cm^{-1})}$$

and

$$Q = u \frac{(C_s - \overline{C_w})(C_s - \overline{C_c})}{G^2}, \frac{mW}{m^2 - sr - cm^{-1}} \quad (7.3.3-3)$$

where u is a predetermined parameter which will be provided at three principal (or backup) instrument temperatures. The u values at other instrument temperatures will be interpolated from these three principal (or backup) values. For channels 9 through 14 (AMSU-A1-1) two sets of the u parameters are provided; one set is for the primary PLL0#1 and the other one for the secondary PLL0#2. The quantity G varies with instrument temperature, which is defined in Table 7.3-1.

For channels 19 and 20 of AMSU-B, the monochromatic assumption breaks down (e.g. channel 20 spans 16 GHz) and a band correction with two coefficients (b and c) has to be applied. These coefficients modify T_w to give an effective temperature T_w'

$$T_w' = b + cT_w$$

which is then used in the Planck function $B(T_w')$ to calculate the radiances for channels 19 and 20. Radiances for all other channels (in both AMSU-A and -B) are computed from $B(T_w)$. The application of Equation 7.3.3-4 is not necessary for the space temperature since the errors in the monochromatic assumption are negligible for such low radiances. For simplification of application, Equation 7.3.3-1 can be rewritten as,

$$R_s = a_0 + a_1 C_s + a_2 C_s^2, \frac{mW}{m^2 - sr - cm^{-1}} \quad (7.3.3-5)$$

The coefficients a_i (where $i=0, 1$ and 2) can be expressed in terms of R_w , G , $\overline{C_w}$ and $\overline{C_c}$. This can be accomplished by rewriting the right-hand side of Equation 7.3.3-1 in powers of C_s and equates the a_i 's to the coefficients of same powers of C_s . The results are:

$$a_0 = R_w - \frac{\overline{C_w}}{G} + u \frac{\overline{C_w C_c}}{G^2}, \frac{mW}{m^2 - sr - cm^{-1}} \quad (7.3.3-6)$$

$$a_1 = \frac{1}{G} - u \frac{\overline{C_c} + \overline{C_w}}{G^2}, \frac{mW}{(m^2 - sr - cm^{-1})count} \quad (7.3.3-7)$$

and

$$a_2 = u \frac{1}{G^2}, \frac{mW}{(m^2 - sr - cm^{-1})count} \quad (7.3.3-8)$$

These calibration coefficients will be calculated for every scan line at each channel and appended to the Level 1b data. With these coefficients, Equation 7.3.3-5 can be used to obtain the scene radiance R_s . It should be noted that the coefficients defined in Equations 7.3.3-6 to 7.3.3-8 are functions of instrument temperature. Therefore, they are, in general, not constant and should be recalculated for each scan. Users who prefer brightness temperature instead of radiance, can make the simple conversion,

$$T_s = B^{-1}(R_s) \quad (7.3.3-9)$$

where $B^{-1}(R_s)$ is the inverse of the Planck function for a radiance R_s . The T_s is the corresponding brightness temperature (or radiometric temperature). However, the conversion (Equation 7.3.3-9) is not performed in the NOAA Level 1b data. Note that for AMSU-B channels 19 and 20 the band correction coefficients must also be applied as follows:

$$T'_s = \frac{T_s - b}{c} \quad (7.3.3-10)$$

where T'_s corresponds to the brightness temperature of channel 19 or 20.

7.3.4 POST LAUNCH EVALUATION AND CALIBRATION

The procedures and formulas described in the above sections were primarily derived from the pre-launch analysis of the AMSU-A and -B calibration data from T/V chambers. Post launch evaluation and calibration have been extensively carried out with overall favorable results. In one report published by Tsan Mo (1999), the findings showed that the radiometric counts and channel gains correlate linearly with the instrument temperature. The NE(Delta) T values calculated from the AMSU- A 1B data compare favorably to those obtained from the pre- launch test data. All channels on the NOAA-15 AMSU-A have functioned well since its powering up after launch, except Channel 14 which has shown an anomalous behavior since early January 1999. The full report can be accessed from the SPIE Digital Library at <http://proceedings.spiedigitallibrary.org/proceeding.aspx?articleid=994440>.

Numerous products have been created over the years reflecting the success of the AMSU instrument.

7.4 SBUV/2

The objective of the calibration program is to achieve a state-of-the-art calibration of the SBUV/2 instrument including response to spectral radiance, response to spectral irradiance, ratio of radiance-to-irradiance responses, and the temperature dependence of response. Continuity of this calibration has been maintained throughout the series.

7.4.1 SBUV/2 CALIBRATION OVERVIEW

Each SBUV/2 instrument consists of a nadir-viewing double monochromator of the Eber-Fastie type, and a cloud cover radiometer (CCR, a filter photometer). A photomultiplier tube detects light exiting the monochromator. They are designed to measure the ratio of backscattered ultraviolet solar radiance to solar irradiance. The SBUV/2 instruments can measure from 152.71 to 443.35 nm in steps of 0.07 nm with a bandpass of 1.1 nm. During normal operation, the backscattered radiance from the nadir is measured at 12 near-UV wavelengths from 252 to 340 nm about 100 times per orbit on the sunlight portion. Light coming into the instrument is first depolarized to remove instrument sensitivity to the polarized backscattered radiances. The CCR makes measurements at 379 nm with a bandpass of 3 nm, and is used to detect scene reflectivity changes during a scan. A diffuser plate is periodically deployed to measure the solar irradiance at the same 12 wavelengths. The instrument is also equipped with a Mercury calibration lamp to monitor both the wavelength scale of the monochromator grating and any degradation of the diffuser.

SBUV/2 instruments use three overlapping gain ranges to measure the solar and Earth radiation which varies over six orders of magnitude. Gain ranges 1 and 2 originate from the photomultiplier anode, while gain range 3 originates from the cathode which allows direct measurement of the instrument's gain. This design differs from SBUV where the anode was the source of all output ranges. For SBUV/2, measurements from the Earth and sun are output on different electronic gain ranges at shorter wavelengths and high solar zenith angles; therefore the instrument's electronic gain is not always canceled in the albedo ratio. The photomultiplier gain (called the interrange ratio, IRR) must be monitored and carefully evaluated over time for accurate long term measurements.

The objective of the calibration program has been to achieve a state-of-the-art calibration of the SBUV/2 instrument including response to spectral radiance, response to spectral irradiance, ratio of radiance to irradiance responses, and the temperature dependence and linearity of the response. Continuity of this calibration has been maintained throughout the series of the operational instruments. Ozone profiles and total amounts are derived from the ratio of the observed backscattered Earth spectral radiance to the incoming solar spectral irradiance. This ratio is proportional to the Earth's geometrical albedo. The only difference in the radiance and irradiance observations is the instrument diffuser used to make the solar irradiance measurement; the remaining optical components are identical. Therefore, the principle changes in the instrument that result in a change in the measured albedo over time are the diffuser reflectivity and the gain range ratios.

7.4.2 COMPONENT CALIBRATION

The spectral efficiency of each optical component of the SBUV/2 instrument is measured by the suppliers in the course of their acceptance testing. This demonstrates that specifications have been met. Also, it allows prediction of the eventual spectral transmittance of the system. If there is a need, the component efficiency tests can be repeated. Monitor (witness sample) mirrors accompany the instrument optics throughout the program and will be periodically tested for spectral reflectivity.

At the subsystem level of assembly, additional procedures and tests are carried out that support

the final calibration. The depolarizer is tested by measuring the residual polarization of initially polarized light after it has passed through the depolarizer. System linearity and dynamic range tests are done before the calibration lamp and diffuser assemblies are installed. Wavelength calibration, bandpass, instrument profile and spectral resolution tests are done with the calibration lamp installed, but before the diffuser assembly is installed. After integration of the complete instrument, but before the formal verification testing begins, a series of checks are run during which final adjustments are made. During this process, the optical alignment is measured and adjusted if necessary, and all field-of-view (FOV) related tests performed, since the same fixture is used for all FOV related tests. FOV test include: size, shape and uniformity of both monochromator and CCR (cloud cover radiometer or photometer) fields and their coincidence. Out-of-band rejection and stray light tests are conducted at this stage. Finally, the first radiance/irradiance response tests are run in air, establishing a baseline to which subsequent tests can be compared.

During environmental testing, after the vibration sequence, the radiance/irradiance response in air is measured and the alignment and FOV checks are made. The definitive radiometric calibration is done just prior to T/V testing. During T/V, the spectral radiometric calibration is extended to the required temperature plateaus and down to 160nm using the Vacuum Test fixture (VTF). The calibration transfer standard sources are returned to NIST for recalibration as necessary to allow the closest possible interpolation between standardizations. During T/V testing, the monochromator wavelength scale change with temperature, if any, is measured.

7.4.3 RADIANCE AND IRRADANCE CALIBRATION

In calibrating the Earth Viewing (radiance) mode of operation, the target seen by the instrument is a calibrated reflectance diffuser illuminated by collimated light from a NIST calibrated source of spectral irradiance. The absolute value of the radiance of the test diffuser is a function of the same source irradiance, the efficiencies of the intervening components and their geometries.

In calibrating the radiance-to-irradiance ratio, the set-up is fixed and the test diffuser and the instrument diffuser are alternately placed in the light path. The filter detector monitor measures relative irradiance I the incoming beam in three broad wavelength bands centered around 180, 250 and 300 nm. If the filter detector monitor and the instrument indicate a decrease in signal from all light sources, the windows and collimating mirrors are checked for efficiency. By swinging the filter detector monitor so that it views the diffuser, a relative efficiency measurement of either diffuser can be obtained. In this way, any changes in the diffusers can be detected during testing. The filter detector monitor uses a quartz windowed bi-alkali photodiode, the type used for the detectors. It is used for relative monitoring measurements only.

The instrument is designed to respond in proportion to the spectral radiance, ($\text{mW}\cdot\text{m}^{-2}\cdot\text{sr}^{-1}\cdot\Delta^{-1}$) incident upon its entrance slit. The area of the entrance slit, the FOV is defined by the field stop, and the bandpass of the monochromator determine the radiant flux, $M(W)$, which enters the system. The system transmission efficiency determines the radiance flux at the photocathode. The quantum efficiency and gain of the detector system determine the final response to a given input. To calibrate this system, standard sources of spectral irradiance that will produce a certain

spectral irradiance ($\text{mW}\cdot\text{m}^{-2}\cdot\text{sr}^{-1}\cdot\Delta^{-1}$) at a given distance under carefully controlled conditions are available.

The approach taken is to use a standard (NIST secondary) spectral irradiance to illuminate a diffuser whose bidirectional reflectance distribution function (BDRF) is accurately known. A collimating mirror is used to achieve a uniformity of irradiance and of angle of illumination at the diffuser. Thus, at given angles of view, the spectral radiance of the diffuser is known, and the instrument response to this radiance is measured. The problem is that all three elements (window, collimating mirror and diffuser) have been interposed between the standard source and each introduces changes into the transfer process. The window and collimating mirror can be measured for spectral transmission and reflectance to within 3% to 1 % errors. This is done before and after each major calibration sequence. In addition, the filter detector monitor will indicate any general change in collimator or diffuser efficiency. Extensive experiments and analysis have demonstrated that radiometric calibration are precise to better than 1% (2Φ). The absolute accuracy of the BDRF values is 3%. Non-linearities, wavelength errors and other instrument factors have uncertainties that are less than 1%.

The test diffuser efficiency is measured by direct comparison to a NIST calibrated standard. This is done in the calibration test fixture using the instrument as the detector. A mask in the collimated beam with a 2.5 cm (1 in) aperture will restrict illumination to a small area of the test diffuser. The NIST standard diffuser is moved in from of the test diffuser so that its efficiency is mapped over it surface.

With the standards of irradiance, the collimator and the test diffuser, the instrument is presented with a diffuse source of known radiance against which its response can be calibrated. To calibrate the irradiance mode of operation, the test diffuser is moved out of the way as the instrument diffuser is deployed. In effect, this compares to the efficiencies of the two diffusers, since their interchange is the only difference in the two measurements.

The result of the radiometric calibration is a function that assigns a calibration constant, K_E , for irradiance to each instrument wavelength, λ , given by:

$$K_E(\lambda) = \frac{E_{dk}(\lambda)}{CC_E(\lambda)} \quad (7.4.3-1)$$

where E_{dk} is the test fixture irradiance, and CC_E is the corrected count rate or instrument signal. Similarly, the calibration constant for radiance, K_L , is given by:

$$K_L(\lambda) = \frac{L_{dk}(\lambda)}{CC_L(\lambda)} \quad (7.4.3-2)$$

where E_{dk} is the test fixture radiance and CC_L is the corrected count rate or instrument signal.

Integrating spheres are also used to calibrate the SBUV/2 instruments. Comparison of integrating sphere and diffuser calibrations has shown agreement of about 1% for Space Shuttle SBUV (SSBUV) and SBUV/2.

The SBUV/2 instrument has four viewing modes (nadir Earth, solar diffuser, lamp diffuser, and lamp direct), but only two are used for radiometric calibration. In orbit, the instrument has a nadir view of the Earth in radiance mode. During ground testing, the sensor module views an illuminated target. In the irradiance mode, the sensor module deploys a reflective diffuser, which is illuminated by the Sun during a portion of the orbit. In ground tests, the diffuser is illuminated by a collimated source. The instrument has two major grating modes for collecting radiance and irradiance data. The first is the step scan mode when 12 channels are scanned from 252 to 340 nm in 32 seconds. The second is the continuous scan (160 nm to 405 nm) mode used for solar irradiance and wavelength calibration. So, there are 4 sets of calibration constants, namely: radiance discrete mode, irradiance discrete mode, radiance continuous mode and irradiance continuous mode.

7.4.4 ADDITIONAL INSTRUMENT CALIBRATION

The spectrometric testing and calibration of the monochromator is done as a subsystem in that the diffuser and depolarizer at the front end are installed. The instrument entrance slit is illuminated via an integrating sphere by various intense line sources and the line positions versus grating positions are recorded. One of the sources is the in-flight Mercury calibration lamp. The integrating sphere fills the optical extent of the monochromator for these tests.

Further calibration information is obtained on the diffuser and gain ranges. The brightness of the diffuser varies with wavelength and illumination angle of the source. A series of measurements of FEL lamp and Mercury Pen Ray lamp are made over the range of expected solar illumination and viewing angles to characterize the diffuser goniometry. The interrange ratios are determined by the ratio of counts in two gain ranges when both ranges have valid data. They are observed to vary as a function of wavelength.

Out-of-band errors are measured pre-flight by viewing the diffuse sky or a diffuser illuminated by the sun at the earth's surface. Tests of current instruments resulted in larger responses in the region below 290 nm than the expected signals would produce. Additional measurements to estimate signal to noise, stray light, out-of-field response, alignment, and stability have been made and are presented in various papers since the launch of NOAA-K.

Full details of each instrument's calibrations are presented in the Specifications and Compliance Calibration Data Books (see Ball 1991) prepared by the instrument contractor.

7.4.5 IN ORBIT CALIBRATION

Once in orbit, the SBUV/2 responses are carefully monitored over time. Hilsenrath et al.(1995) have shown that measured albedo relative to the "day 1" albedo over time is a function

of true change in Earth radiance, diffuser degradation, and interrange ratio (PMT gain). Since the primary measurements are ratios, changes in many of the components will cancel. The diffuser plate is used only for the solar irradiance measurements. Accurate characterization of its degradation is required to maintain calibration. This is accomplished by using an on-board Hg calibration lamp. The lamp is alternately viewed directly and indirectly by illuminating the diffuser. Diffuser degradation is monitored at six mercury lines spanning 185 to 405 nm.

The wavelengths associated with the grating positions have been observed to drift. Measurements of the calibration lamp at the six mercury lines, and continuous scans of the solar spectrum (via the diffuser) are used to estimate this drift. Absolute wavelength accuracy can be determined to about 0.02 nm.

The three gain ranges evolve differently over time, and must be periodically renormalized to each other. This can be accomplished by using measurements for which two ranges are valid. The magnitude of the interrange ratios (gain range 2 versus gain range 3) for the SBUV/2 on NOAA-11 decreased by about 15% over its 5 years of operation.

7.5 SEM-2

The SEM-2 TED and MEPED are calibrated with proton and electron beams to provide the direct channel responses. Proper instrument operation in-orbit is verified by In-Flight (IFC) cycles, which verify electronic gains, thresholds, channel logic and detector noise levels. The TED particle calibration and IFC operation is described in Section 7.5.1, while the MEPED particle calibration and IFC is described in Section 7.5.2.

7.5.1 TED CALIBRATION

7.5.1.1 TED Particle Calibration

The TED ESAs are all calibrated with electron and ion beams to provide measured values for the geometric factors. This corrects for the variations in absolute CDEM detection efficiency, and requires that a unique set of calibration constants for each TED be used in processing the telemetered data. Each TED has a Calibration Report which provides all of the necessary calibration constants.

The primary TED measurements are the electron and proton (ion) energy fluxes measured at 0 and 30 degrees to the local vertical. The energy fluxes are measured for 0.05 to 1 keV and for 1 to 20 keV, so there are 8 primary energy flux values and calibration constants. Approximate values for the conversion of telemetered energy flux counts into energy are listed in Table 7.5.1.1-1. Note that the 8-bit telemetry count is a compressed count, and must first be converted into an uncompressed count. The actual calibrated constants for a given TED may differ by as much as 50% from the values listed in Table 7.5.1.1-1.

Table 7.4.1.1-1. Nominal Values for TED Energy Flux Calibration Factors.				
Channel Designation	Particle Type	Direction Measured	Energy Range (keV)	Calibration Factor (erg/(cm²-s-sr-count))

0EFL	Electrons	0	0.05 - 1	2×10^{-6}
0EFH	Electrons	0	1 - 20	5×10^{-5}
3EFL	Electrons	30	0.05 - 1	2×10^{-6}
3EFH	Electrons	30	1 - 20	5×10^{-5}
0PFL	Protons (Ions)	0	0.05 - 1	1×10^{-6}
0PFH	Protons(Ions)	0	1 - 20	4×10^{-5}
3PFL	Protons (Ions)	30	0.05 - 1	1×10^{-6}
3PFH	Protons(Ions)	30	1 - 20	4×10^{-5}

The TED also provides four point energy spectra and a measurement of the peak flux point in the spectrum for each particle type/measurement direction. The four point spectra require a total of 16 calibration constants to convert the telemetered counts, after decompression, into particle energy fluxes. The peak flux channel can be any of the 16 channels measured for a given particle type/measurement direction, and requires the full set of channel calibration factors, a total of 64 constants. These calibration constants are obtained from the Calibration Report for the TED, and may vary by 50% from the nominal values.

7.5.1.2 TED In-Flight Calibration

Each of the eight CDEMs has a threshold set to one of four values with each design value twice the previous one, as shown in Table 7.5.1.2-1.

Level	Binary Level	Designed Value Voltage
0	00	0.2375 V
1	01	0.475 V
2	10	0.950 V
3	11	1.900 V

The threshold rejects low level noise which appears in the signal processing circuitry. Natural signal pulses from the CDEN are normally larger than the highest threshold so any threshold can be used. At the beginning of life, the lowest threshold is used. If noise appears, it can be rejected by choosing a higher threshold. In addition, CDEM gain may down with age. This is expected to show up with the highest threshold where weaker pulses may not be counted. This effect can be corrected by used a higher CDEM operating voltage, selected by ground command.

TED In-Flight Calibration (IFC) starts on command from the ground. Because the IFC changes settings, the settings in use before the IFC starts are remembered and are restored when the TED IFC terminates. Settings commanded from the ground during TED IFC are remembered and are the ones “restored” on termination. TED IFC has two phases, phase 0 and phase 1, both controlled by the DPU.

Phase 0 measures the thresholds using one major frame (32 seconds). This is done with increasing pulses in at the CDEM with the Electrostatic Analyzers (ESAs) turned off so no natural pulses occur. In eight seconds, the calibration pulses rise in a linear series of steps to

2.50 V at the discriminator, exceeding the highest of the four thresholds. This is done four times, once for each of the four thresholds, taking a total of 32 seconds.

Phase 1, which starts at the end of Phase 0, measures CDEM detection efficiency. Phase 1 has no calibration pulses but the ESAs are turned back on so that operation is normal except that the thresholds are cycled through their four levels (0,1,2,3,0,...). It runs for about one spacecraft orbit (189 x 32 second major frames = 100.8 minutes). This allows natural pulses to exercise all thresholds thereby testing the CDEMs as well as the signal processing circuitry. A full revolution is used to assure that there will be pulses, most of which appear in the auroral region. Data from this phase of the IFC is used to determine if any CDEMs have degraded, and if any CDEM operating voltage adjustments are required.

7.5.2 MEPED CALIBRATION

7.5.2.1 MEPED Particle Calibration

The MEPED telescopes are calibrated with proton and electron beams at a number of accelerators, covering the energy range from 20 keV to several MeV. The omnidirectional sensors were calibrated with proton beams over the range of 13 MeV to 153 MeV. The calibrated particle response geometric factors for the telescopes are listed in Table 7.5.2.1-1. Note that the electron channels have a secondary response to protons which has the same geometric factor. The listed geometric factors for particles in the appropriate energy range. The proton channels also have a small response to high energy electrons, which is primarily in the 0P1 and 9P1 channels. The electron geometric factor of the 0P1 and 9P1 channels varies from about 10^{-7} cm²-sr at 30 keV to 10^{-6} cm²-sr at 100 keV at 300 keV to 10^{-4} cm²-sr at 2MeV.

Table 7.5.2.1-1. MEPED Telescope Calibrated Geometric Factors.			
Channel Designation	Particle Type	Detected Energy Range (keV)	Geometric Factor G(cm²-sr)
0E1 and 9E1	Electrons	>30	0.0100
0E2 and 9E2	Electrons	>100	0.0100
0E3 and 9E3	Electrons	>300	0.0100
0E1 and 9E1	Protons	210-2700	0.0100
0E2 and 9E2	Protons	280-2700	0.0100
0E3 and 9E3	Protons	440-2700	0.0100
0P1 and 9P1	Protons	30-80	0.0100
0P2 and 9P2	Protons	80-250	0.0100
0P3 and 9P3	Protons	250-800	0.0100
0P4 and 9P4	Protons	800-2500	0.0100
0P5 and 9P5	Protons	2500-6900	0.0100
0P6 and 9P6	Protons	>6900	0.0100

The calibrated proton geometric factors for the four omnidirectional sensor channels are given in Table 7.5.2.1-2, which lists the measured angular responses integrated over the angular range of 0 to 105. This corresponds to the approximate loss + reflected particle cone over the polar caps,

where the omnidirectional sensor measurements of solar proton fluxes are expected to be most important. The omnidirectional sensors have detector energy loss thresholds of 2.5 MeV, which effectively eliminates any response to electrons and electron bremsstrahlung. This produces a nominal upper limit of about 500 MeV for detected protons, which is moderately broad because of energy loss straggling and variations of particle path in the detector with angle position.

Table 7.5.2.1-2. MEPED Omnidirectional Sensor Calibrated Geometric Factors.			
Channel Designation	Particle Type	Detected Energy Range (MeV)	Geometric Factor G(cm²-sr)
P6	Protons	16 - > 500	1.50 (See Note 1.)
P7	Protons	35 - > 500	1.50 (See Note 1.)
P8	Protons	70 - > 500	1.50 (See Note 1.)
P9	Protons	140 - > 500	1.50 (See Note 1.)
Note:			
1. Geometric factors integrated over the angle range of 0 to 105, which includes most of the particle-filled cone over the Polar caps.			

The thresholds and combinatorial logic with determine the various particle energy channels are calibrated for each MEPED using radioactive sources with precise x-ray energies. The telescope detectors are calibrated against the 59.54 keV x-ray from ²⁴¹Am, which produces a strong photo-peak in the measured spectrum. This is used to calibrate a precision Pulse Generator, which is then used to calibrate all the threshold levels. The omnidirectional sensor detectors and thresholds are calibrated using the 661.6 keV gamma-ray from ¹³⁷Cs, which produces a strong Compton edge at 477.3 keV. This Compton edge is used to calibrate the precision Pulse Generator, which in turn is used to calibrate detector gain and threshold level values. All MEPED detectors are selected to have the same sensitive thickness and detection area, so the calibrated particle responses for all MEPEDs should be identical.

7.5.2.2 MEPED In-Flight Calibration

The MEPED In-Flight Calibration (IFC) is an automatic calibration verification started by command from the ground. Processing the telemetered data gives the energy of each threshold and the full width at half maximum (FWHM) noise for the telescope detectors. After the command, the IFC starts at the next Major Frame sync pulse from the spacecraft. The IFC terminates automatically, but may also be terminated by command. The DPU controls the IFC cycle, which is used to verify all of the electronic gains, threshold values, and coincidence logic for the MEPED.

During the IFC negative pulses at a frequency of 2080 Hz are applied to the front end of each charge-sensitive amplifier. The amplitude (voltage) of the pulses is stepped up in a linear staircase of 0 to 191 steps. Groups of four pulse amplitudes are counted and telemetered, making 48 values received on the ground. The MEPED IFC has two phases, 0 and 1. The pulses are scaled for each detector and IFC phase. Phase 0 measures low energy thresholds and telescope detector noise widths, and phase 1 measures high energy thresholds. The fraction of the maximum count (account of all pulses if the pulse height is well above the threshold) for a given

IFC output is called F. For Phase 0 the variation of F with IFC pulse amplitude is fit with a Gaussian distribution to determine both the threshold value and the detector FWHM noise. For Phase 1 there is generally only one value of F which is between 0 and 1, and this value is used to measure the threshold.

The threshold values used in the MEPED are listed in Table 7.5.2.2-1, which shows which threshold is used for the lower energy determination of the listed particle channels. The IFC Phase used for each threshold measurement is also listed. Note that all telescope thresholds are actually two separate values, one for the 0 telescope and one for the 90 telescope. Thresholds for the “E” channels are for the electron telescopes, while thresholds for the “P” channels are for the proton telescopes.

The actual thresholds are derived from the IFC count data using calibration factors obtained from the calibrated threshold values for each MEPED. The MEPED IFC calibration factors are provided in a Calibration Report for each instrument.

Table 7.5.2.2-1. MEPED Thresholds and IFC Phase for Measurement

Threshold Designation	Threshold Values (keV)	Particle Channels	IFC Phase	FWHM Noise Measurement
LS1(2 levels)	25.6	0E1 and 9E1	0	Yes
LS2(2 levels)	98.1	0E2 and 9E2	0	Yes
LS3(2 levels)	299.	0E3 and 9E3	1	No
LS4(2levels)	2500.	0E3 and 9E3	1	No
LS1(2 levels)	21.4	0P1 and 9P1	0	Yes
LS2(2 levels)	70.7	0P2 and 9P2	0	Yes
LS3(2 levels)	243.	0P3 and 9P3	1	No
LS4(2 Levels)	796.	0P4 and 9P4	1	No
LS5(2 levels)	2498.	0P5 and 9P5	1	No
LS6(2 levels)	50.	0P6 and 9P6	0	Yes
LS1(omni)	2500	P6	1	No
LS2(omni)	2500	P7	1	No
LS3(omni)	2500	P8	1	No
LS4(omni)	2500	P9	1	No

7.6 MICROWAVE HUMIDITY SOUNDER (MHS)

The launch of NOAA-18 (NOAA-N) on May 20, 2005 presented a new challenge to product production due to a new instrument, the Microwave Humidity Sounder (MHS), which replaced the AMSU-B flown on NOAA-15, -16, and -17 satellites. A major difference between MHS and AMSU-B (both five channel radiometers) is the measurement frequency at channel 2 and channel 5. MHS has 157 GHz and 190 GHz while AMSU-B operates at 150 GHz and 183, +/- 7 GHz.

The MHS has nominal and redundant Platinum Resistance Thermometers (PRTs) built into the

instrument. One set each of five PRTs and three calibration resistors is routed to the telemetry acquisition circuit of the Processor and Interface Electronics A (PIE-A) and PIE-B, respectively. MHS also has nominal and redundant local oscillators, Side-A and Side-B. One of the sets is used for nominal and the other set will serve as backup. A more thorough description of the MHS instrument can be found in Section 3.9.

7.6.1 COMPUTATION OF PRT TEMPERATURES

The PRT temperatures are derived in a two-step process. First the PRT counts in the MHS data packets are converted to resistance R (in ohms) using three reference resistor values which are in the data packets (in counts). Subsequent conversion of PRT resistance R into PRT temperature is accomplished using a cubic polynomial of the form,

$$T_k = \sum_{j=0}^3 f_{kj} R_k^j \quad (7.6-1)$$

where T_k and R_k represent the temperature and resistance of the PRT k , respectively. The coefficients f_{kj} will be provided for each PRT. MHS has five PRTs (per PIE) mounted on the underside of the onboard calibration target (OBCT). Each PRT is sampled once per scan and these PRT counts are output in the science data packet. The PRT count must be converted into resistance R_k which appears in Equation 7.6.1-1. The process of converting the PRT counts into resistance is described in the next section.

7.6.2 THREE PRT CALIBRATION CHANNELS

MHS has three PRT calibration channels which provide data for a linear count-to-resistance conversion that is updated in each scan. These are precision resistors whose values are known to high precision over their operating temperatures and life. Their values are chosen to lie at the upper, middle, and lower resistance ranges expected of the OBCT PRTs throughout mission life. These three resistors are referred to as the PRT Calibration channels 1, 2, and 3 (PRT CAL n , where $n=1, 2,$ and 3), respectively. Their values in counts are measured once per scan and are output in the science data packet. The resistance of the PRT CAL n is assumed to be a linear function of the PRT CAL n counts,

$$R_{CALn} = \alpha + \beta C_{CALn} \quad (7.6.2-1)$$

where R_{CALn} and C_{CALn} represent the resistance and count of the PRT CAL n , (with $n=1, 2,$ and 3) respectively. The α and β are the offset and slope. For each scan, the C_{CALn} values are measured and the R_{CALn} values, which remain constant, are provided for each MHS flight model. Therefore, the α and β can be obtained by a least-square fit from Equation 7.6.2-1. The results are,

$$\alpha = \frac{\left(\sum_{n=1}^3 R_{CALn} \right) \left(\sum_{n=1}^3 C_{CALn}^2 \right) - \left(\sum_{n=1}^3 C_{CALn} \right) \left(\sum_{n=1}^3 C_{CALn} R_{CALn} \right)}{3 \left(\sum_{n=1}^3 C_{CALn}^2 \right) - \left(\sum_{n=1}^3 C_{CALn} \right)} \quad (7.6.2-2)$$

$$\beta = \frac{3 \left(\sum_{n=1}^3 C_{CALn} R_{CALn} \right) - \left(\sum_{n=1}^3 R_{CALn} \right) \left(\sum_{n=1}^3 C_{CALn} \right)}{3 \left(\sum_{n=1}^3 C_{CALn}^2 \right) - \left(\sum_{n=1}^3 C_{CALn} \right)} \quad (7.6.2-3)$$

7.6.3 CONVERSION OF PRT COUNTS INTO RESISTANCE

For each scan, these α and β values are computed and then applied to each OBCT PRT to convert the OBCT PRT count C_k into resistance R_k as follows,

$$R_k = \alpha + \beta C_k \quad (7.6.3-1)$$

where R_k and C_k are the resistance and count, respectively, of the PRT k with $k=1$ to 5. The R_k will be used in Equation 7.6.1-1 for calculation of the OBCT PRT temperatures, T_k , values of which are output to the MHS Level 1b data.

7.6.4 BLACKBODY TEMPERATURE

The mean OBCT temperature, T_w , is calculated from the individual PRT temperatures,

$$T_w = \frac{\sum_{k=1}^m W_k T_k}{\sum_{k=1}^m W_k} + \Delta T_w \quad (7.6.4-1)$$

where $m=5$ represents the number of OBCT PRTs (as listed in Table 3.9.2.1-2) and W_k is a weight assigned to each PRT k . The quantity T_w represents a warm load correction factor, which is derived for each channel from the pre-launch test data at three instrument temperatures (low, nominal, and high). The procedure for determining the T_w values is described in Mo (1996). The W_k value, which equals 1 (0) if the PRT k is determined good (bad) before or after launch. For the central PRT, $W_k=2$ will be assigned.

Similarly, a cold space temperature correction, ΔT_c , may be required. This is due to the fact that the space view may be contaminated by radiation which originates from the spacecraft and the Earth's limb. Thus, the effective cold space temperature is given by:

$$T_c = 2.73 + \Delta T_c \quad (7.6.4-2)$$

where 2.73K is the cosmic background brightness temperature and ΔT_c will be determined from pre- or post-launch data analysis. The ΔT_c values of individual channels and each of the possible space viewing directions will be provided for each MHS flight model in Appendix D.

7.6.5 MHS HOUSEKEEPING THERMISTORS AND CURRENT MONITORS

7.6.5.1 Standard Thermistors

There are 24 Housekeeping (HK) thermistors which monitor the temperatures at various MHS telemetry points, such as amplifiers, and local oscillators. These data, which are primarily for instrument health and safety monitoring, are not used in the radiometric retrieval algorithm of science data. The accuracy of these HK temperatures is less rigorous than that of the PRT temperatures. The 24 HK thermistors use a common set of conversion coefficients. The two-step process of converting counts to resistance and resistance to temperature can be compressed into a single step with negligible errors. This single step process computes the thermistor temperatures directly from the thermistor counts, using a polynomial of the form,

$$T_{th} = \sum_{n=0}^4 g_n C_{th}^n \quad (7.6.5.1-1)$$

where T_{th} and C_{th} represent the temperature and count of the thermistors, respectively. The C_{th} is also referred to as the 8-bit code from the Thermistor Telemetry. The coefficients g_n , which are valid for -40°C to 60°C (i.e., 243 K to 333 K), will be provided for each MHS flight model in Appendix D.

7.6.5.2 Current Monitors

There are six current monitors that measure the current consumption of various power lines in the MHS instrument. The measured output in count C_I is converted to current, I (in amperes) by a linear relationship as follows,

$$I = I_0 + mC_I \quad (7.6.5.2-1)$$

where I_0 is the intercept and m denotes the slope, respectively. Values of I_0 and m will be provided for each monitor in Appendix D.

7.6.5.3 Survival Thermistors

In the MHS analog telemetry, there are three survival thermistors which monitor the temperatures of the Receiver, Electronics Equipment, and Scan Mechanism. These survival

thermistors are powered to provide measurements even when the instrument power is off.

The conversion of the survival thermistor counts into temperatures is accomplished by a polynomial of the form,

$$T_{SUR} = \sum_{m=0}^5 h_m V^m \quad (7.6.5.3-1)$$

where $V = 0.02 \times \text{Count}$ represents the measured output in volts. One set of coefficients h_m applies to all three survival thermistors.

7.6.6 CALIBRATION ALGORITHM

The calibration algorithm from Mo (1996) that converts the Earth scene counts C_s to radiance, R_s , is given as follows,

$$R_s = R_w + (R_w - R_c) \left(\frac{C_s - \overline{C_w}}{\overline{C_w} - \overline{C_c}} \right) + Q \quad (7.6.6-1)$$

where R_w and R_c are the radiance computed from the OBCT temperature T_w and the effective cold space temperature T_c , respectively, using the Planck function. The C_s is the radiometric count from the Earth scenes. The $\overline{C_w}$ and $\overline{C_c}$ are the convoluted blackbody count and space counts, respectively, as defined in Equation 7.6.6-3 below. The quantity Q , which represents the nonlinear contribution, is given by,

$$Q = u(R_w - R_c)^2 \frac{(C_s - \overline{C_w})(C_s - \overline{C_c})}{(\overline{C_w} - \overline{C_c})^2} \quad (7.6.6-2)$$

where u is a free parameter, values of which are determined at three instrument temperatures (low, nominal, and high) from the pre-launch calibration data. After the launch of MHS, the u value at an actual on-orbit instrument temperature will be interpolated from these three pre-launch values.

For each scan, C_w represents the mean blackbody radiometric count of the four samples of the blackbody target. Similarly, C_c represents the mean space radiometric count of the four samples of space viewing. To reduce noise in the calibrations, the CX (where $X=W$ or C) for each scan line were convoluted over several neighboring scan lines according to a weight function,

$$\overline{C}_x = \frac{\sum_{i=-n}^n w_i C_x(t_i)}{\sum_{i=-n}^n w_i} \quad (7.6.6-3)$$

where t_i (when $i \neq 0$) represents the time of the scan lines just before or after the current scan line and t_0 is the time of the current scan line. The variable t_i can be written as: $t_i = t_0 + i\Delta t$, where $\Delta t = 8/3$ seconds for MHS. The $2n+1$ values are equally distributed about the scan line to be calibrated. Following the NOAA KLM operational preprocessor software, the value of $n=3$ is chosen for MHS. A set of triangular weights, 1, 2, 3, 4, 3, 2, and 1 are chosen for the weight factor w_i that appears in Equation 7.6.6-3 for the seven scans at $i = -3, -2, -1, 0, 1, 2, \text{ and } 3$, respectively.

For MHS channel 19, the monochromatic assumption breaks down and a band correction with two coefficients has to be applied. These coefficients modify T_w to give an effective temperature T_w' :

$$T_w' = b + cT_w \quad (7.6.6-4)$$

which is then used in the Planck function to give an accurate radiance. The application of Equation 7.6.6-4 is not necessary for the space temperature since the errors in the monochromatic assumption are negligible for such low radiance.

7.6.7 CALIBRATION QUALITY CONTROL

Quality control (QC) in the MHS calibration is very important for producing accurate calibration coefficients in the NESDIS operational calibration process. A scan-by-scan QC process can detect bad data which are flagged in the Level 1b data sets. All of the QC processes that have been built into the NESDIS operational AMSU-B preprocessor are to be included in this MHS algorithm. These and additional QC items are listed as follows,

Intra-scan test of blackbody counts C_w : If any two samples differ more than a preset limit of the blackbody count variation ΔC_w , the $C_w(t_i)$ should be excluded in Equation 7.6.6-3 by setting $w_i=0$.

Intra-scan test of the space counts C_c : If any two samples differ more than a preset limit of the space count variation ΔC_c , the $C_c(t_i)$ should be excluded in Equation 7.6.6-3 by setting $w_i=0$.

Inter-scan test of PRT temperatures T_k : If a T_k differs by more than 0.2K from its value in the previous (good) scan line, the T_k should be omitted from the average in Equation 7.6.4-1 by setting $w_k=0$.

Test of antenna pointing accuracy: If an antenna position reading is out of a preset limit, then an error flag will be set in the Level 1b data.

Radio frequency interference (RFI) correction: It was observed that the transmitters on the NOAA KLM spacecraft can produce serious RFI to the AMSU-B data. A corrective algorithm was developed for correction of the RFI in the AMSU-B. The same algorithm will also be used in the MHS calibration algorithm. Detailed description of the AMSU-B RFI corrective algorithm is online in Appendix M.

Detection and exclusion of the Lunar contaminated space samples from the calibration: Calculate the angular separation between the Moon and each viewing direction of the four space samples. Reject those samples that are within a pre-defined angular threshold (default = 1.5°). In the worst case, three samples may be rejected in this process (keep the sample that has the largest separation angle if all four samples fall within the pre-defined angular threshold). Description of how to calculate the angular separation between the Moon and the space viewing direction is given in Kigawa and Mo (2002). Store the calculated separation angles.

Inter-scan test of sudden jump (or drop) of C_w and C_c : Such sudden change in C_w and C_c has been observed in the NOAA-17 AMSU-A data. A corrective algorithm from Mo (2002) was developed for correction of the effect of such sudden change in the calibration counts on the calibration coefficients.

7.6.8 NOAA LEVEL 1b DATA

The NOAA Polar Orbiter Level 1b data are raw data that have been quality controlled and assembled into discrete data sets, to which Earth location and calibration information are appended but not applied. For simplification of application, Equation 7.6.6-1 can be rewritten as,

$$R_s = a_0 + a_1 C_s + a_2 C_s^2 \quad (7.6.8-1)$$

where the calibration coefficients a_i (where $i = 0, 1, \text{ and } 2$) can be expressed in terms of R_w , G , $\overline{C_w}$ and $\overline{C_c}$. This is accomplished by rewriting the right-hand side of Equation 7.6.6-1 in powers of C_s and equating the a_i 's to the coefficients of same powers of C_s . The results are,

$$a_0 = R_w - \frac{\overline{C_w}}{G} + u \frac{\overline{C_w} \overline{C_c}}{G^2} \quad (7.6.8-2)$$

$$a_1 = \frac{1}{G} - u \frac{\overline{C_c} + \overline{C_w}}{G^2} \quad (7.6.8-3)$$

and

$$a_2 = u \frac{1}{G^2} \quad (7.6.8-4)$$

where G represents the channel gain and is defined as

$$G = \frac{\overline{C_w} - \overline{C_c}}{R_w - R_c} \quad (7.6.8-5)$$

These calibration coefficients will be calculated at each scan line for all channels and appended to the Level 1b data. With these coefficients, one can simply apply Equation 7.6.8-1 to obtain the scene radiance R_s . Users, who prefer brightness temperature instead of radiance, can make the simple conversion,

$$T_s = B^{-1}(R_s) \quad (7.6.5-6)$$

where $B^{-1}(R_s)$ is the inverse of the Planck function for radiance R_s . The T_s is the converted brightness temperature.

For MHS channel 19, the band correction must be taken into consideration in the inverse process as follows,

$$T_s = \frac{B^{-1}(R_s) - b}{c} \quad (7.6.8-7)$$